Morphology of Quench Condensed Pb Films near the Insulator to Metal Transition

K. L. Ekinci and J. M. Valles, Jr.
Department of Physics, Brown University, Providence, Rhode Island 02912
(Received 20 August 1998)

We present *in situ* scanning tunneling microscopy topographs of Pb films, formed by vapor deposition onto cold ($T < 20$ K), inert substrates, near their insulator to metal transition. At the critical mass deposited thickness for conduction, $d_G \cong 5.2$ nm, the films consist of approximately two layers of nanoclusters with diameter, $2r \approx 20$ nm and height, $3.5 \leq h \leq 5.5$ nm. We discuss how the nanocluster size and formation mechanism dictate the need for two layers to form in order for conduction to commence. [S0031-9007(99)08430-6]

PACS numbers: 71.30.+h, 68.55.Jk, 73.61.At

As the mass per unit area of a film of metal on an insulating substrate increases, it makes a transition from an insulating (dc resistance, $R_{\rm dc} = \infty$) to a metallic ($R_{\rm dc} =$ finite) phase. The physical factors that control this transition depend strongly on how the film grows and its resulting structure. A simple example is encountered for Au vapor deposited on warm substrates ($T_S \geq 700$ K). Islands nucleate on the substrate, grow laterally, coalesce, and create a conduction path that percolates across the film [1]. By contrast, the processes controlling the conduction onset in films deposited on cold, inert substrates ($T_S \approx 4$ K)—the so-called *granular* quench condensed (QC) films—are poorly understood and have been a source of controversy [2–4]. The primary obstacle has been the lack of direct information about their mode of growth and corresponding structure. Nevertheless, QC films have been used in numerous studies of superconductivity [2,5], localization [6,7], and quantum phase transitions [3,8].

Figure 1 provides an example of an insulator to metal transition in a QC film system, with Pb films on an oxidized amorphous Ge substrate (GeO_x) [9]. Like other systems, these films become conducting, hence, metallic, only after a finite mass deposited thickness of material, $d_G \cong 5.2$ nm has been quench condensed. After conduction is initiated, the film sheet resistance R_S decreases exponentially with additional increments of material. There are two different interpretations of this behavior. The more commonly accepted of the two depicts a film at d_G as composed of islands, higher than d_G. Interisland electron tunneling controls the transport, and the tunnel gaps decrease linearly with the amount of deposited material [2,3]. The opposing interpretation questions the existence of islands in QC films [4]. Thermally activated mechanisms for island growth freeze out at cryogenic temperatures. Adatoms are believed to stick where they land [4,10–12] and, consequently, QC films are expected to form in a structurally continuous amorphous phase when only a few atomic layers thick. The exciting claim that this phase is microscopically insulating emerges because $d_G \approx 20$–30 atomic monolayers $\gg$ few monolayers. At d_G, metallic grains grow within the amorphous matrix, and conduction ensues through intergrain tunneling [4].

Recent *in situ* scanning tunneling microscopy (STM) experiments [13] on granular QC Au and Pb films show that their morphology changes dramatically with thickness and exhibits features that are similar to those proposed in *both* models. The thinnest films lack structure, containing no grains or islands, and thus, qualitatively resemble the conjectured amorphous phase. Above a critical thickness, $d_c \sim 1$–2 nm (4–8 atomic monolayers) for Pb, the films form in an islanded morphology. The thickest films are polycrystalline with small platelet shaped grains. Moreover, similar results on several substrates prepared differently show that QC film structure is independent of the substrate material and cleanliness.

In this paper, we present *in situ* STM and transport measurements which establish that at d_G, the films are polycrystalline with two nearly complete layers of grains,

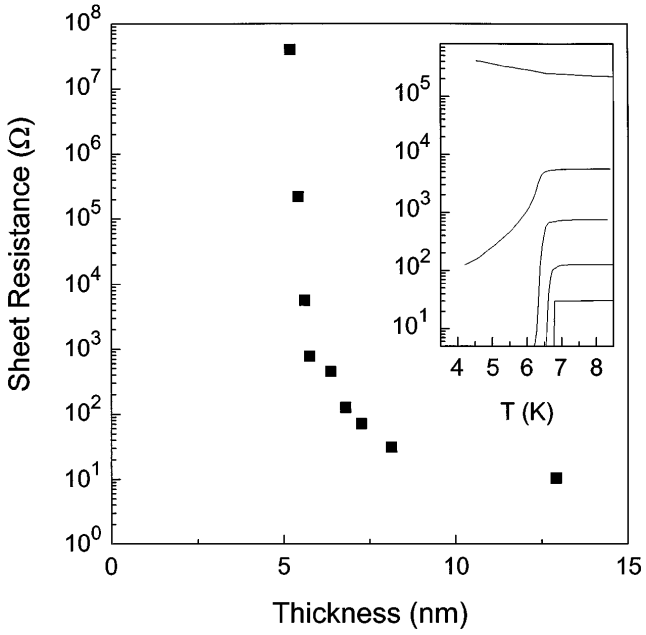

FIG. 1. Sheet resistance, R_S at 8 K vs thickness d for Pb films deposited on GeO_x. The inset shows the temperature dependence of R_S for five of these films. The film thicknesses in the inset can be traced by comparing the R_S values at 8 K to the R_S vs d curve.

 0031-9007/99/82(7)/1518(4)$15.00

contrary to *both* conduction onset models. We discuss how the mode of growth and the size of the grains prevent the islanded phase from conducting and require the existence of a second layer of grains for conduction. The results are consistent with, but do no demonstrate, the existence of the microscopically insulating phase.

For both the transport and STM experiments, the cryostat chamber [14] containing the substrate and the thermal evaporation sources was cooled to cryogenic temperatures by direct immersion in liquid helium, after it was evacuated to a pressure, $P < 2 \times 10^{-7}$ Torr. We estimate that the cryopumping action of the chamber walls reduced P to $<10^{-10}$ Torr except during evaporation. High purity Pb (99.999%) was evaporated at a rate of 0.1–1 Å/s as measured by a quartz crystal microbalance from a resistively heated tungsten filament that had been outgassed behind a shutter. The substrate temperature, as measure by a carbon resistance thermometer, increased to $\approx$13 K during evaporation. Transport measurements were performed using a 4-terminal contact configuration and lock-in techniques.

Figure 1 displays a typical insulator to metal transition for a granular QC film. Pb was deposited continuously onto an insulating GeO_x substrate until the film exhibited a measurable conductance. Further incremental depositions were made and the resistance of each film was measured as a function of temperature (see Fig. 1 inset). As noted earlier, the film resistance initially decreases exponentially with thickness. The inset also shows that d_G and the onset thickness for superconduction, d_{SC}, coincide closely, $d_{SC} - d_G \approx 0.6$ nm in agreement with past measurements [3,15,16].

We carried out our most detailed film morphology measurements using highly oriented pyrolytic graphite (HOPG) substrates. These substrates present large flat surfaces that are ideal for determining the Pb film structure and conduct, which is essential for imaging insulating Pb films. We performed two additional sets of experiments which showed that the evolution of the film morphology on HOPG is the same as on GeO_x. First, we obtained STM topographs of Pb films on a GeO_x substrate with a conducting underlayer for direct comparison (see later discussion). Second, we measured d_{SC} for Pb films on HOPG and found it to agree with that on GeO_x. Eleven Pb films with $3.0 \leq d \leq 13.9$ nm were deposited incrementally on HOPG and the resistance of the parallel combination of the HOPG and Pb film, $R_{\|}$, was measured down to 4.2 K. $R_{\|}$ dropped abruptly when the Pb film became superconducting, and we define T_c as the temperature at which the sheet resistance of the film dropped below 10 Ω. As shown in Fig. 2, T_c increases abruptly above 4.2 K at a film thickness, $d = 5.8$ nm and rises slowly with increasing d. A similarly defined T_c for the Pb on GeO_x (Fig. 2) exhibits identical behavior implying that the Pb film morphologies on the two substrates are the same at d_{SC}. Moreover, the conducting HOPG substrate does not influence the Pb film superconducting transition for $T \geq 4.2$ K [17].

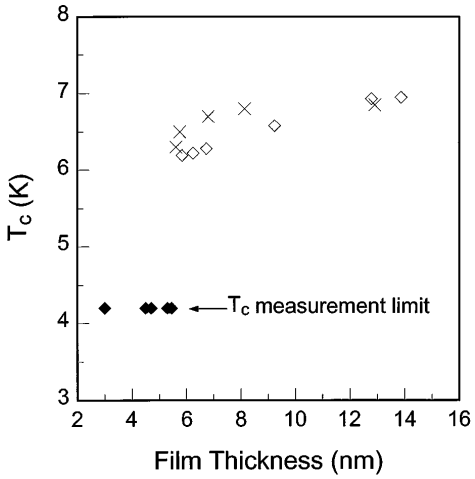

FIG. 2. T_c vs thickness for QC Pb films on HOPG (diamonds) and GeO_x (crosses).

Topographs of two films which do not superconduct above 4.2 K ($d = 3.0$ and 4.8 nm) and one which does ($d = 6.1$ nm) are exhibited as Fig. 3. The thinnest film [Figs. 3(a) and 3(b)] consists of a single layer of Pb grains with a relatively narrow size distribution that uniformly covers the flat areas of the substrate. Some grains are isolated while others are members of small clusters of grains. There are gaps between these clusters, where line scans (not shown) expose the flat HOPG substrate. Tip resolution effects [18], however, make the apparent gap sizes smaller than actual. Measured from the flat substrate between grains, the grains have heights $3.5 \leq h \leq 5.5$ nm with an average $\langle h \rangle = 4.1$ nm. Using the grain density, the average grain height, and the deposition thickness, we estimate the average grain diameter to be 20 nm and that Pb covers 75% of the HOPG surface. With the deposition of additional Pb (+1.8 nm), grains with the same dimensions as those in the first layer appear on top of the first layer of grains [Figs. 3(c) and 3(d)]. Fewer gaps are apparent compared to the $d = 3.0$ nm film suggesting that the new grains tend to grow over the gaps [13]. Further addition of 1.3 nm makes the second layer of grains appear approximately as densely packed [see Figs. 3(e) and 3(f)] as the grains in the $d = 3.0$ nm film. Thus, conduction and superconduction appear in films with approximately two layers of grains.

Finally, for direct comparison, we present an STM image of a nonconducting Pb film with $d = 3.0$ nm on a 2.5 nm thick GeO_x layer [Fig. 4(a)]. Beneath the GeO_x layer was a 11 nm thick Au layer that provided a conducting path for the tunneling electrons to leave the film [Fig. 4(b)]. A single layer of Pb grains of the same dimensions as those in Fig. 3(a) is evident in Fig. 4(a). This image and others of thicker films (not shown) imply that the Pb film morphology is the same on the two substrates. This result is consistent with previous STM measurements [13] and past observations of the formation of electrically identical QC films on a variety of inert substrates such as

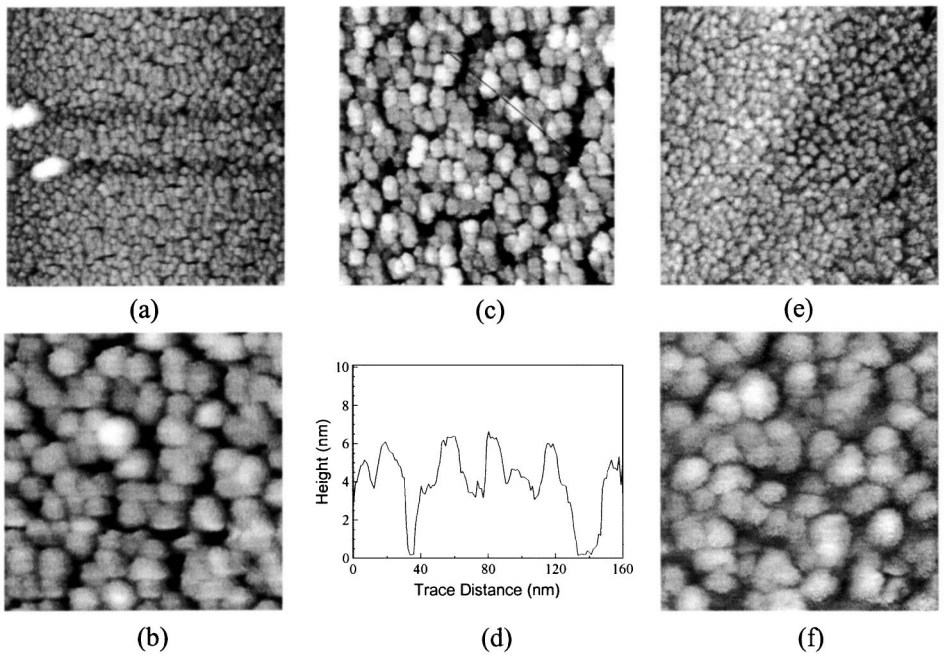

FIG. 3. *In situ* STM images of a QC Pb film on HOPG as its thickness d is varied for a transition from an insulating to a metallic phase. (a),(b) $d = 3.0$ nm. Scan areas 675×675 nm (a) and 130×130 nm (b). (c) $d = 4.8$ nm. Scan area 240×240 nm. (d) A cross section of the film in (c). (e),(f) $d = 6.1$ nm. Scan areas same as those in (a) and (b). A plateau edge on the substrate is apparent in (e). The gray scale height range is set to $\approx$5.0 nm for all images.

AlO_x [15], glass [15,16], and quartz [19]. In contrast to the Pb films on HOPG, for which images could be obtained using a tunneling voltage as low as 5 mV, it was necessary to apply a tip to sample voltage in excess of 0.2 V to acquire the image in Fig. 4(a). Presumably, electrons attempting to tunnel onto grains on the insulating substrate encounter a Coulomb blockade [20]. An estimate of the charging energy for isolated grains of the size in the film, $E_C = e^2/2C = 0.2$ eV with the single grain capacitance, $C \cong 4\pi\varepsilon_0 V^{1/3}$, determined using the measured grain volume V, supports this idea. Also, images of a conducting $d = 6$ nm film on GeO_x could be obtained at voltages at least as low as $V_T = 5$ mV.

Our results imply that the morphology at d_G in granular QC films differs substantially from earlier proposals. First, the precursor phase turns into a metallic granular phase ($d_c \sim 1$–2 nm [13]) long before the onset of electrical conduction ($d_G \cong 5.2$ nm) contrary to the conjecture [4] that conduction begins as the precursor phase turns into a metallic phase. We hasten to add that it is still not clear [13] whether the insulating behavior of the precursor phase is intrinsic [4] or is due to cracks in the film. Second, despite the fact that metallic islands in Fig. 3(b) cover 75% of the substrate area, well above the 2D percolation threshold of 50% [21], they do not form a continuous electrical path across the film. Thus, a simple percolation analysis cannot account for the onset of conduction in films grown on cold ($T < 20$ K) substrates.

We attribute the insulating behavior in the thinnest films to a few factors. First, the precursor film phase is believed to be less dense than the grains that form from it [4,13]. Thus, in the process of grain formation, the film shrinks in volume and becomes islanded. We estimate the average size of the gaps between islands as $\langle \delta_{GG} \rangle \approx 1.2$ nm in the 3.0 nm film of Fig. 3(a) assuming the grains cover 75% of the substrate, are equal, and are regularly arranged. For two grains, which are roughly the dimensions of the ends of STM tips, this distance corresponds to an estimated tunneling resistance in excess of 1 GΩ. Second, the grains are so small that at $T \cong 4$ K, $E_C \gg kT$ and charges cannot be thermally activated to overcome interisland Coulomb blockades.

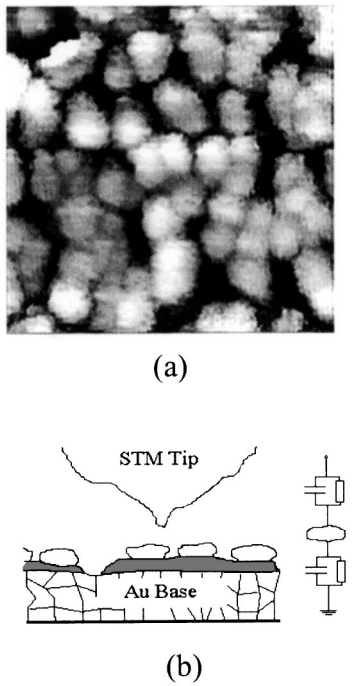

FIG. 4. (a) *In situ* STM image of a $d = 3.0$ nm thick QC Pb film on GeO_x. The scan area is 92×92 nm. (b) Drawing of the substrate and the equivalent circuit. Regions of the Au as large as 250×250 nm were covered uniformly by the Ge with an rms roughness $\approx$0.7 nm.

The upper grains in a thicker film [cf. Fig. 3(c)] create low resistance paths between the lower layer grains, forming electrically connected multigrain clusters and reducing the number of tunnel junctions in the film. The clusters have larger perimeters, which enhance tunneling rates. E_C for a cluster is reduced from the single grain E_C by a factor that scales as $1/N^{\nu}$, where N is the number of grains in a cluster, and $1/3 \leq \nu \leq 1/2$ for simple models [22] of the capacitance. In order for $kT > E_C/N^{\nu}$ the clusters must consist of more than 10^4 grains. Thus, if conduction first occurs via tunneling [3,19], then it is not surprising that nearly a complete layer of bridging grains is required before conduction commences.

While interesting details of the film growth process remain unclear, our observations support a proposed qualitative growth model [11,13]. In that model, an amorphous structure results after the deposition of the first few monolayers and this structure *avalanches* into crystalline grains through local amorphous to crystalline transformations [23]. This process repeats to form the second layer of grains [24]. This picture accounts for (1) the conduction onset thicknesses coinciding closely for films deposited incrementally on HOPG and continuously on GeO_x, and (2) the STM images, to within our resolution, being similar for conducting films of $d \approx 6.0$ nm regardless of their deposition history.

STM topographs of QC granular Pb films reveal an unexpected morphology at their insulator to metal transition. Our previous STM measurements on Au films suggest that this morphology is general [13]. Knowledge of the morphology will directly benefit physical descriptions of the wide range of phenomena explored using these films. For example, models for the insulator to superconductor transition in 2D (see Ref. [8], for example), the insulator to metal transition in the 1D limit [25], and the temperature dependence of the transport in just conducting films [3] all rely on an accurate picture of film structure.

We have benefited from discussions with A. Truscott, M. Strongin, and A. Vandelay. This study was supported by the NSF through DMR-9296192, DMR-9502920, and partially by ONR by N00014-95-0747.

[1] D. W. Pashley *et al.*, Philos. Mag. **10**, 127 (1964).
[2] M. Strongin *et al.*, Phys. Rev. B **1**, 1078 (1970).
[3] R. C. Dynes, J. P. Garno, and J. M. Rowell, Phys. Rev. Lett. **40**, 479 (1978).
[4] A. V. Danilov *et al.*, Phys. Rev. B **51**, 5514 (1995); A. V. Danilov *et al.*, J. Low Temp. Phys. **103**, 1 (1996).
[5] W. Buckel, Z. Phys. **138**, 136 (1954).
[6] G. Bergmann, Phys. Rep. **107**, 1 (1984).
[7] D. J. Huang, G. Reisfeld, and M. Strongin, Phys. Rev. B **55**, R1977 (1997).
[8] H. M. Jaegar *et al.*, Phys. Rev. B **34**, 4920 (1986).
[9] A 12 nm Ge film was deposited on glass at room temperature and oxidized in air prior to cool down.
[10] S. Fujime, Jpn. J. Appl. Phys. **6**, 305 (1967); Y. F. Komnik, Sov. J. Low Temp. Phys. **8**, 1 (1982).
[11] C. R. M. Grovenor, H. T. G. Hentzell, and D. A. Smith, Acta Metall. **32**, 773 (1984).
[12] D. E. Sanders and A. E. DePristo, Surf. Sci. **254**, 341 (1991).
[13] K. L. Ekinci and J. M. Valles, Jr., Acta Mater. **46**, 4549 (1998); Phys. Rev. B **58**, 7347 (1998).
[14] K. L. Ekinci and J. M. Valles, Jr., Rev. Sci. Instrum. **68**, 4152 (1997).
[15] S. Y. Hsu and J. M. Valles, Jr., Phys. Rev. B **49**, 16 600 (1994).
[16] I. L. Landau, I. A. Parshin, and L. Rinderer, J. Low Temp. Phys. **108**, 305 (1997).
[17] As a layered zero gap semiconductor, HOPG is expected to have weak proximity interactions with the Pb islands. In support of this, A. Truscott *et al.* observed a superconducting energy gap identical to the bulk value in a 10 nm thick Pb film on HOPG (private communication). The proximity effect cannot be responsible for the abrupt rise in T_c displayed in Fig. 2. The increase of T_c from 0 K to the bulk value, in a film of superconducting material in the proximity of a metal ought to occur gradually with film thickness. The weakness of the proximity effect between Pb and HOPG also indicates that Josephson coupling through the substrate will be negligible for $T \geq 4.2$ K.
[18] For a more detailed discussion of tip effects in STM imaging of QC films, see [13] and H. Reiss *et al.*, Appl. Phys. Lett. **57**, 867 (1990).
[19] R. P. Barber, Jr. and R. Glover III, Phys. Rev. B **42**, 6754 (1990).
[20] M. Amman, S. B. Field, and R. C. Jaklevic, Phys. Rev. B **48**, 12 104 (1993).
[21] D. Stauffer, *Introduction to Percolation Theory* (Taylor and Francis, London, 1985).
[22] We roughly estimate the range of ν from the following. For an isolated cluster we presume that $C \propto (\text{volume})^{1/3} \propto N^{1/3}$. For one cluster surrounded by clusters, the capacitance will be determined by the area of the perimeter of that cluster and the distance between its perimeter and its neighbors. Because the clusters have a flat aspect ratio, the cluster radius and, hence, the perimeter scales as $N^{1/2}$ and $C \propto N^{1/2}$.
[23] An appropriate surface growth model for very low substrate temperatures would be in the extreme kinetic limit of pure random deposition with negligible relaxation. It would give rise to amorphous films with a rough surface characterized, in the limit of no relaxation, by a Poisson distribution of heights. These film structures, however, are metastable and our experiments suggest that past a certain film thickness, they are unstable to the formation of crystallites.
[24] Once grains have formed, STM probing would not be sensitive to the upper amorphous blanket as the tip would primarily follow the contours generated by the lower grains.
[25] A. V. Herzog *et al.*, Phys. Rev. Lett. **76**, 668 (1996).